

Defense Nuclear Nonproliferation Research & Development
Nuclear Explosion Monitoring Program Review
NEM 2019

Material and Gas Transport Properties of Test Bed Core

Kristopher Kuhlman
Sandia National Laboratories

March 20th, 2019 09:20

- Sandia National Laboratories Team
 - Applied Systems Analysis and Research: Kris Kuhlman
 - Geomechanics: Scott Broome, PI; Joshua Feldman; Jason Heath
 - Geochemistry: Matthew Paul
- Laboratory studies were conducted on representative core samples in the vicinity of the Barnwell and P-Tunnel sites to characterize mechanical, momentum, and mass transport properties.
 - The mechanical properties Barnwell core samples have been performed.
 - The mechanical properties of P-Tunnel core are in progress.
 - Momentum and mass transport properties of the core have been performed.



- Core Data Sets
 - SAND2019-0786 Diffusive Properties of UNESE Core Samples via Continuously Monitored Mass Spectroscopy
 - FY17 Interim Report, DOE/NV/25946—3411, Appendices 5 and 12.
- Technical Advance
 - Diffusivity Measurements via Continuously Monitored Mass Spectrometry (#14899)

Nilson et al. (1991) provided a conceptual model for how tracer gases may reach the surface despite large depths.

1. The barometer drops. Subsurface gases are drawn towards the surface, predominately through fractures.
2. While the subsurface pressure approaches equilibrium, tracers diffuse from the fractures into the matrix.
3. The barometer rises. Fresh atmospheric gases are pressed into the fractures, but little is pressed into the matrix.
4. While the subsurface pressure approaches equilibrium, tracers diffuses from the matrix back into the fractures.
5. The cycle is repeated, ratcheting the subsurface tracer front towards the surface.

Efficiency depends upon:

- Frequency and magnitude of surface oscillations
- Fracture permeability, aperture, and spacing
- Tracer diffusivity and matrix capacity

Nilson, R.H. et al. 1991. "Atmospheric pumping: A mechanism causing vertical transport of contaminated gases through fractured permeable media". *J Geophys. Res.* 96: 21933-48

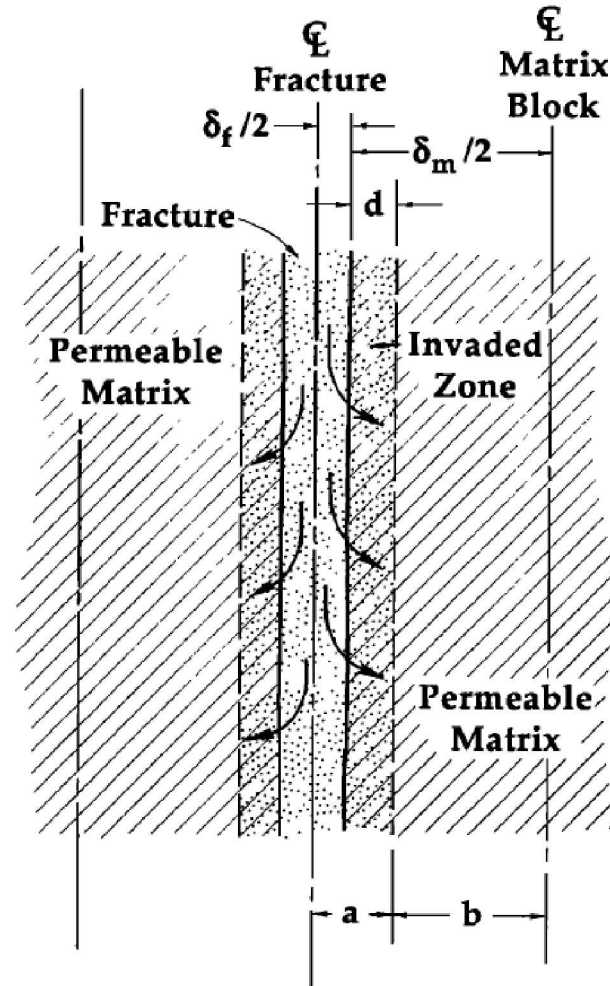


Fig. 11. Schematic of fresh air invading a fractured permeable medium during an increase in barometric pressure. Invasion depth d is accommodated by a slight compression of gas within matrix blocks.

Fundamentals of longitudinal dispersion

- Viscous shearing results in a parabolic velocity profile
- Lateral diffusivity blunts the contaminant front
- Asymptotic behavior is Gaussian as per CLT

Taylor-Aris dispersion is additive with but inversely proportional to molecular diffusivity.

Similar behavior at low frequency pulsatile flow:

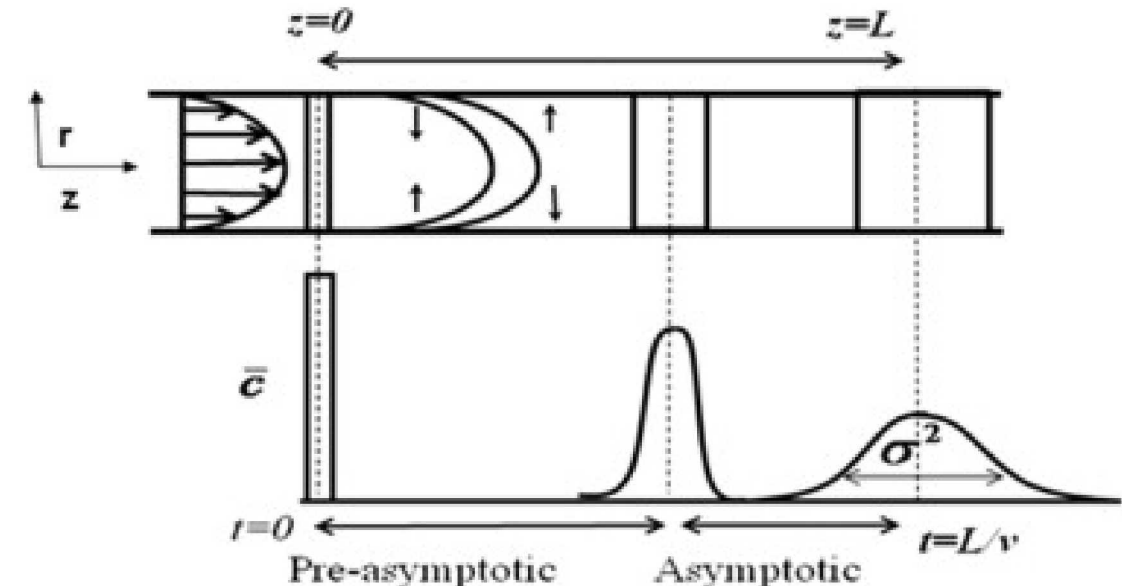
- The peak centroid position oscillates, however
- The contaminant front broadens with each cycle

Similar mechanism for dual-porosity system:

- Fracture/matrix permeability results in greater shearing
- Matrix diffusivity dominates lateral transport

Taylor, G. I. 1953. "Dispersion of soluble matter in solvent flowing slowly through a tube." *Proc. R. Soc. Lond. A* 219: 186-203.

Bhaumik, S.K., Kannan, A., and A. DasGupta 2015. "Taylor-Aris dispersion induced by axial variation in velocity profile in patterned microchannels." *Chem. Eng. Sci.* 96: 251-9.



$$\frac{\partial c_i}{\partial t} + \bar{u}_z \frac{\partial c_i}{\partial z} = K \frac{\partial^2 c_i}{\partial z^2}$$

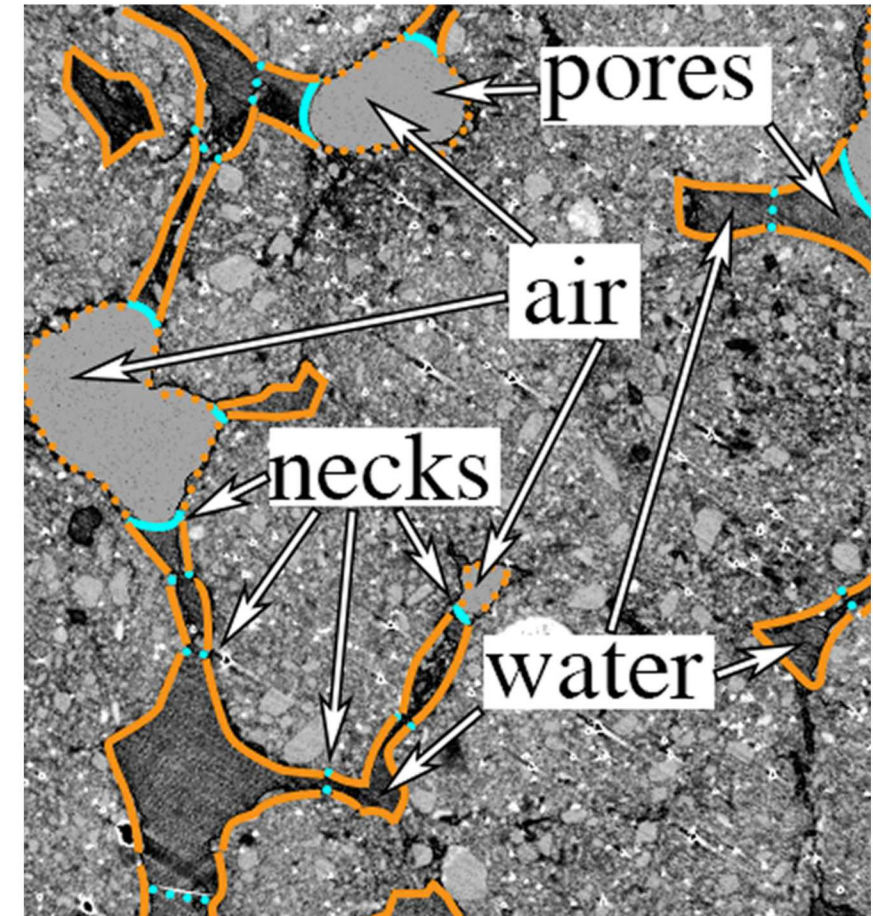
$$K = D_i \left(1 + \gamma \frac{\bar{u}_z^2 r^2}{D_i^2} \right)$$

In all pores, the solid phase is an obstruction:

- Areal porosity ($\bar{\phi}$)
 - Bedded material may have anisotropy
- Gas phase saturation (S_g)
 - Fraction and connectivity of the gas-filled pores
- Tortuosity ($\bar{\tau}$)
 - Advective flow distribution (\bar{u})
 - Frequency of perturbation (ω)

In practice, the effective diffusivity, $\overline{\mathcal{D}}_i$, is the pore diffusivity, \overline{D}_i , times the obstruction factor, \bar{Q} :

$$\overline{\mathcal{D}}_i = D_i \cdot \bar{Q} (\bar{\phi}, S_g, \bar{\tau}(\bar{u}, \omega))$$



Pot, Valerie and P. Baveye 2017. "Research on unsaturated porous media." Cornell.
<http://grainflowresearch.mae.cornell.edu/UnsaturatedPorousMedia/UnsaturatedPorousMedia.html> (accessed January 22, 2019)

Gas diffusion is the result of intermolecular collisions:

- Gas-gas collisions are unaffected by pore walls:
 - Elastic collisions (Maxwell-Stefan diffusion)
- Gas-solid collisions can be:
 - Rebound diffusively (Knudsen diffusion)
 - Surface capture (adsorption + surface diffusion)
- The Dusty-Gas Model includes these interactions:

$$-y_i \frac{\nabla \mu_i}{RT} = \frac{\bar{J}_i}{nD_{iK}} + \frac{\bar{J}_i}{nD_{iS}} + \sum_{j \neq i}^N \frac{y_j \bar{J}_i - y_i \bar{J}_j}{nD_{ij}}$$

- For dilute tracers, the flux is approximately Fickian:

$$\bar{J}_i \cong -D_i \nabla c_i \quad \frac{1}{D_i} = \frac{1}{D_{iK}} + \frac{1}{D_{iS}} + \sum_{j \neq i}^N \frac{y_j}{D_{ij}}$$

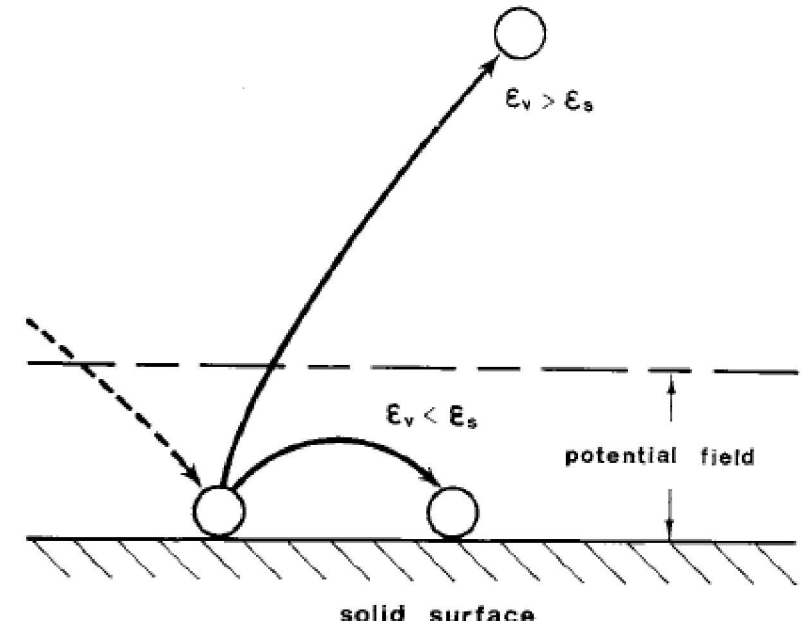


Fig. 1. Schematic view of rebounds of gas molecules on solid surface.

Shindo, Y., T. Hakuta T., H. Yoshitome, and H. Inoue 1983. "Gas diffusion in microporous media in Knudsen's regime." *J. Chem. Eng. Japan* 16:120-6
 Mason, E.A. and A.P. Malinauskas 1983. *Gas Transport in Porous Media: The Dusty-Gas Model*. New York: Elsevier.

Experimental Methods

- Historical options include:
 - Closed Tube (Loschmidt 1870)
 - Evaporation Tube (Stefan 1873)
 - Diffusion Bridge
 - Non-isobaric (Graham 1833)
 - Isobaric (Wicke-Kallenbach 1941)
 - Two-bulb (Ney-Armistead 1947)
- Technical challenges:
 - Must accommodate porous media
 - Noble gases require mass spectrometry
 - Open systems may result in sample dry-out

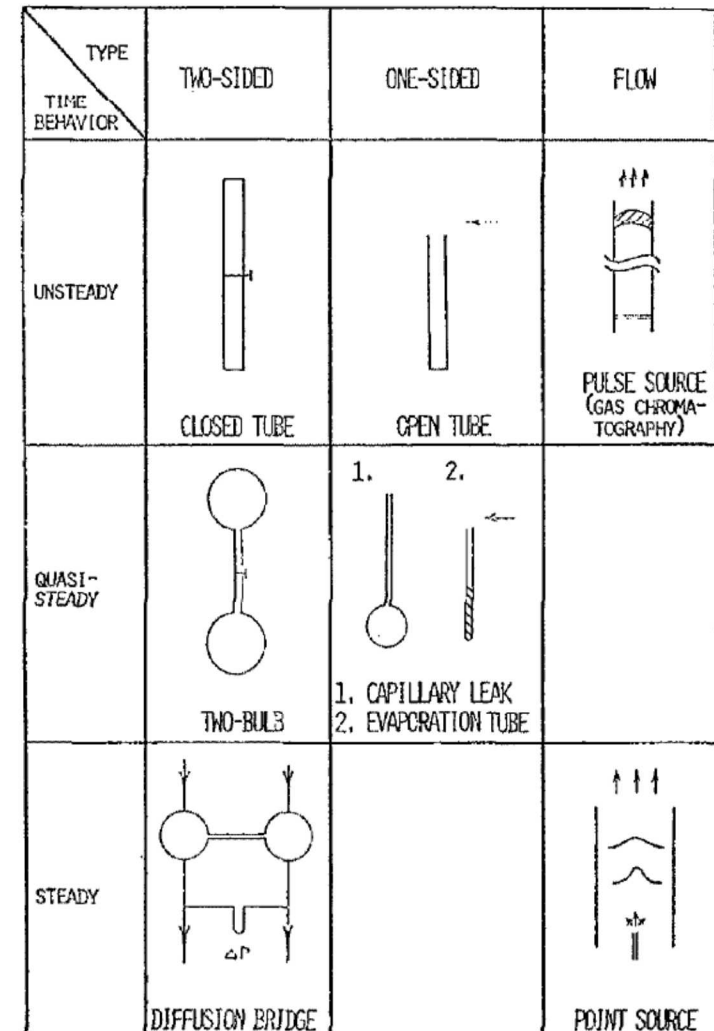


FIGURE 2. Principal experimental methods for diffusion coefficients.

Marrero, T.R. and E.A. Mason 1972. "Gaseous diffusion coefficients." *J. Phys. Chem. Ref.* 1:3-118.1

Ney-Armistead Method through a Capillary

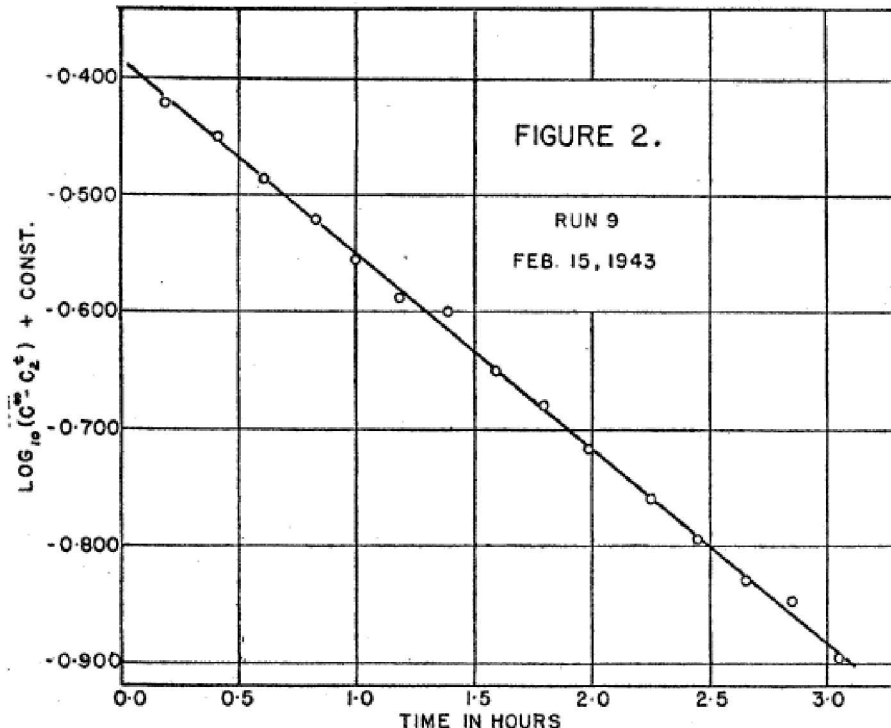


FIG. 2. Graph of $\log_{10}(C^\infty - C_2 t)$ as a function of the time. The slope of the least squares solution, together with the geometrical constants gives the diffusion coefficient.

Ney, E. P. and Armistead, F. C. 1947. "The self-diffusion coefficient of uranium hexafluoride." *Phys. Rev.* 71:14-9.

- Ney and Armistead measured the self-diffusion coefficient of $^{235}\text{UF}_6$ in $^{238}\text{UF}_6$ for the Manhattan project using mass spectrometry.
- The method consists of two gas chambers connected by a restrictive capillary. The small cross sectional area versus chamber volume slows the diffusion rate to be measurable.
- Using known and closed volumes, only one chamber must be monitored.

$$c(t) = c(\infty) - (c(0) - c(\infty))e^{-\gamma t}$$

$$\gamma = -\mathfrak{D}_i \frac{A}{L} \left(\frac{1}{V_1} + \frac{1}{V_2} \right)$$

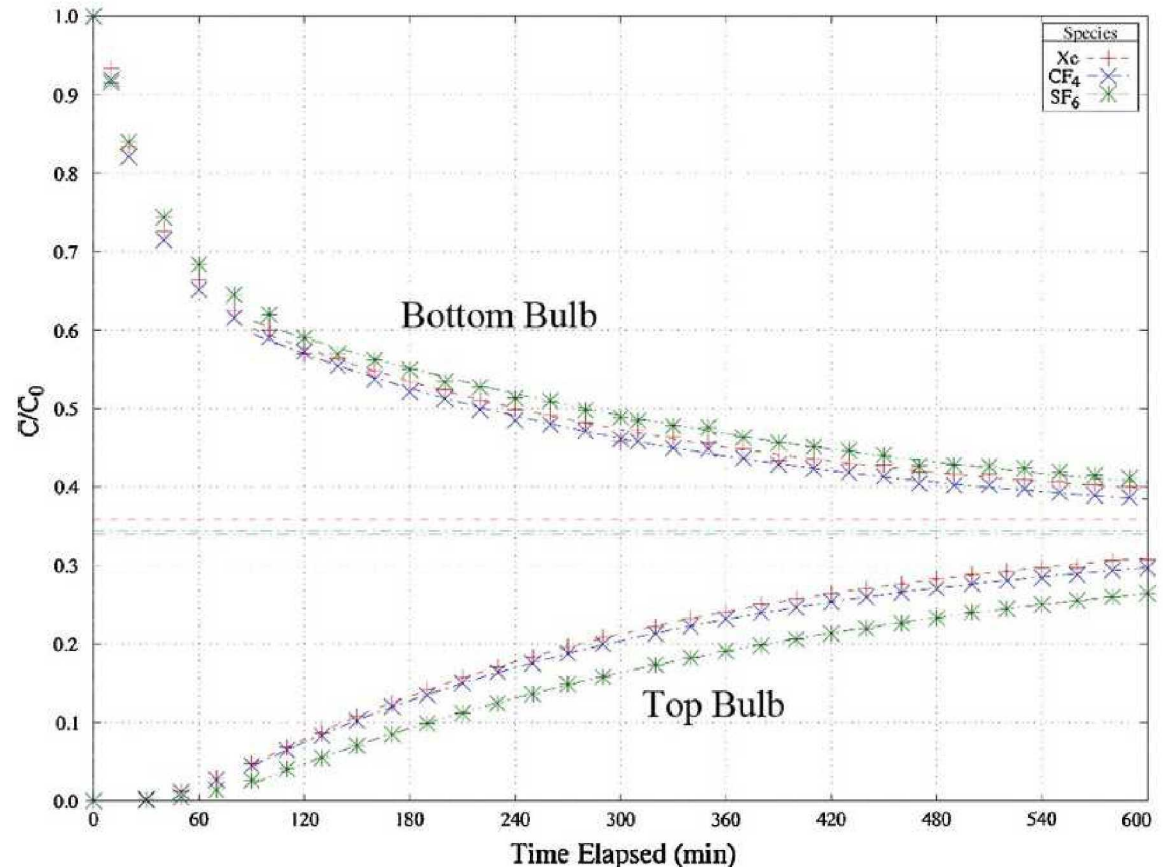
Ney-Armistead Method through Porous Media

When adapted for porous media:

- Accumulation dominants at early times
 - Only the asymptotic data is used
- The equilibrium fraction is unknown
 - Both chambers are sampled to interpolate
- Sampling is either
 - Labor intensive with microsyringes
 - Challenging automation of microfluidics

$$\begin{bmatrix} c_1(t) \\ c_2(t) \end{bmatrix} = c_\infty \begin{bmatrix} 1 \\ 1 \end{bmatrix} + c_\Delta \begin{bmatrix} +V_2 \\ -V_1 \end{bmatrix} e^{-\gamma t}$$

$$\gamma = -\mathfrak{D}_i \frac{A}{L} \left(\frac{1}{V_1} + \frac{1}{V_2} \right)$$

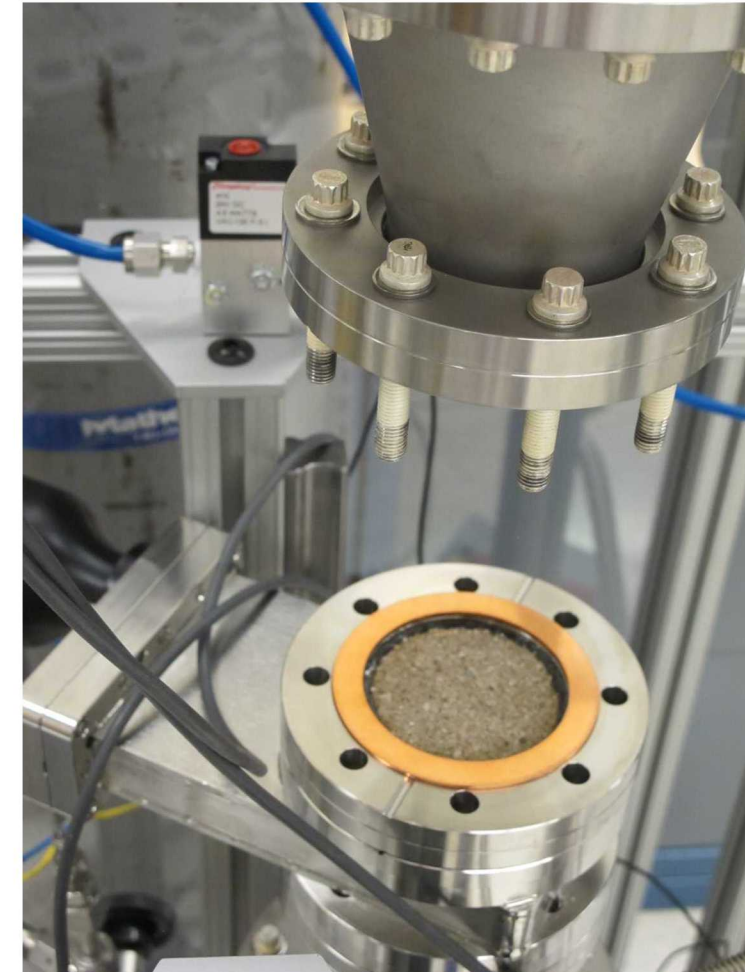


Byers, M.F. et al. 2018. "Evaluation of carbon tetrafluoride as a xenon surrogate for underground gas transport." *J. Radioanal. Nucl. Chem.* 318:465-70.
 Paul, M.J. et al. 2018. "Adsorptive transport of noble gas tracers in porous media." *Int. J. Mod. Phys.: Conf. Ser.* 48:1860124-34.

A new approach was necessary to reduce labor and improve reliability

Relaxing the strict closed system requirement:

- Continuous sampling is supported
 - 1 per second versus 4 per hour
- Microfluidic design is simplified
 - No active components
 - No microsyringe operations
- A new analytical solution is necessary
 - Sampling rate is low but not insignificant
 - Diffusivity is approximated as being constant



Ney-Armistead Method with Continuous Mass Spectrometry

- Flow to the mass spectrometer is limited by Knudsen flow:

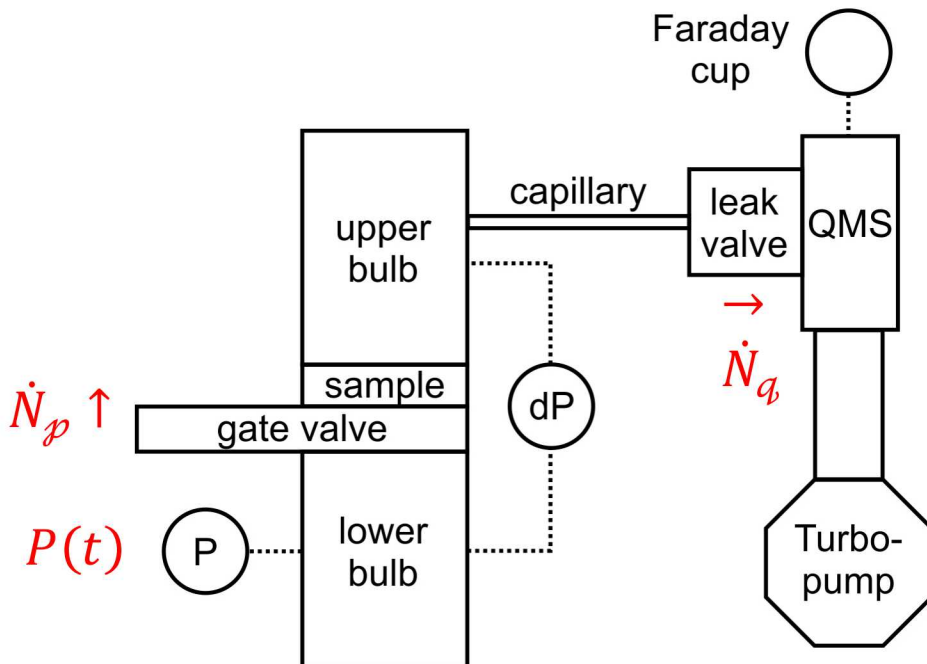
$$\dot{N}_q = c_q \frac{P}{RT}$$

- Flow across porous media sample is in quasi-steady state:

$$\dot{N}_p = \dot{N}_q \frac{V_\ell}{V_\ell + V_u}$$

- At constant temperature, the system pressure decays exponentially:

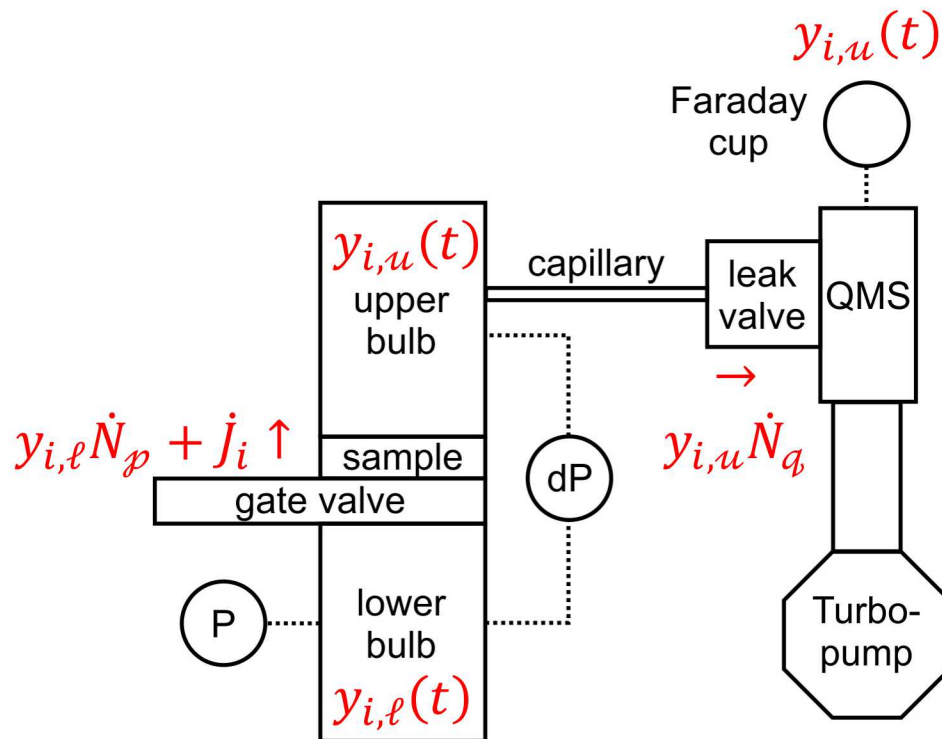
$$P(t) = P(0)e^{-\frac{c_q}{V_1 + V_2}t} = P(0)e^{-k_q t}$$



Paul, M.J. and S. T. Broome 2019. *Diffusive Properties of UNESE Core Samples via Continuously Monitored Mass Spectroscopy*. SAND2019-0786.

Ney-Armistead Method with Continuous Mass Spectrometry

- Tracer-species flux across the sample:



Advection

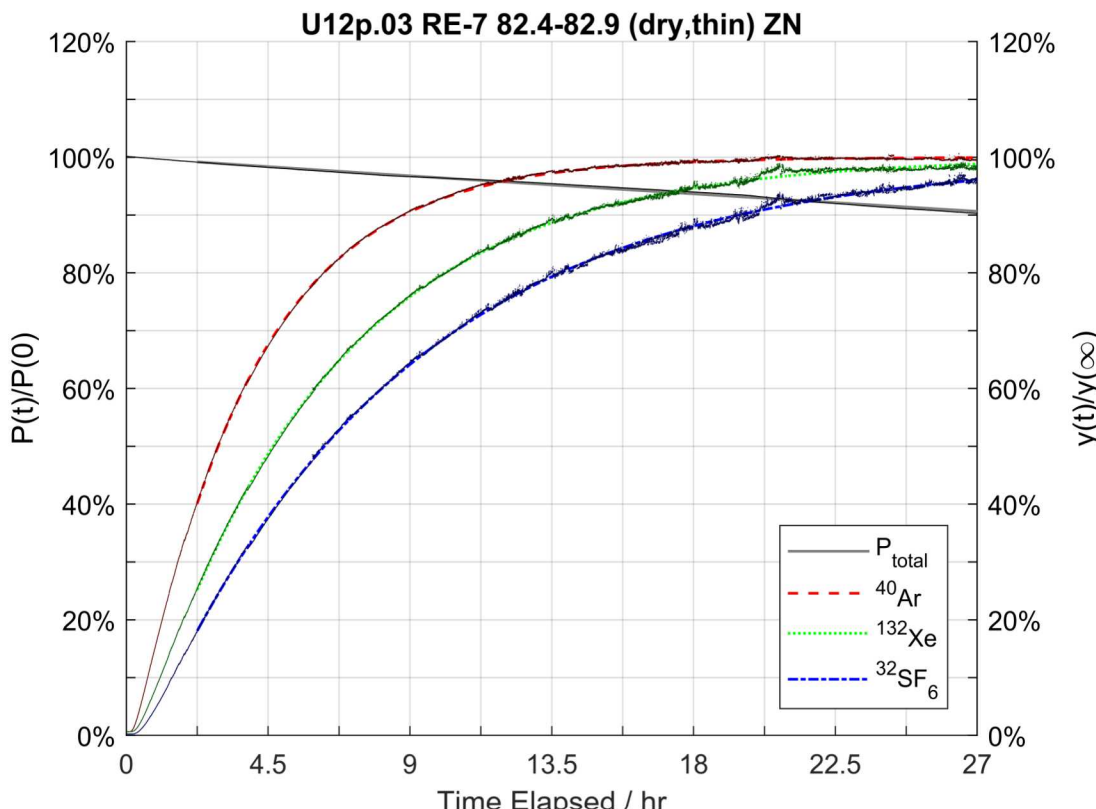
$$y_i \dot{N}_p = k_q V_\ell \frac{P}{RT} y_i \quad j_i = \mathfrak{D}_i \frac{A}{L} \frac{P}{RT} (y_{i,\ell} - y_{i,u})$$

- Solving for the mole fraction:

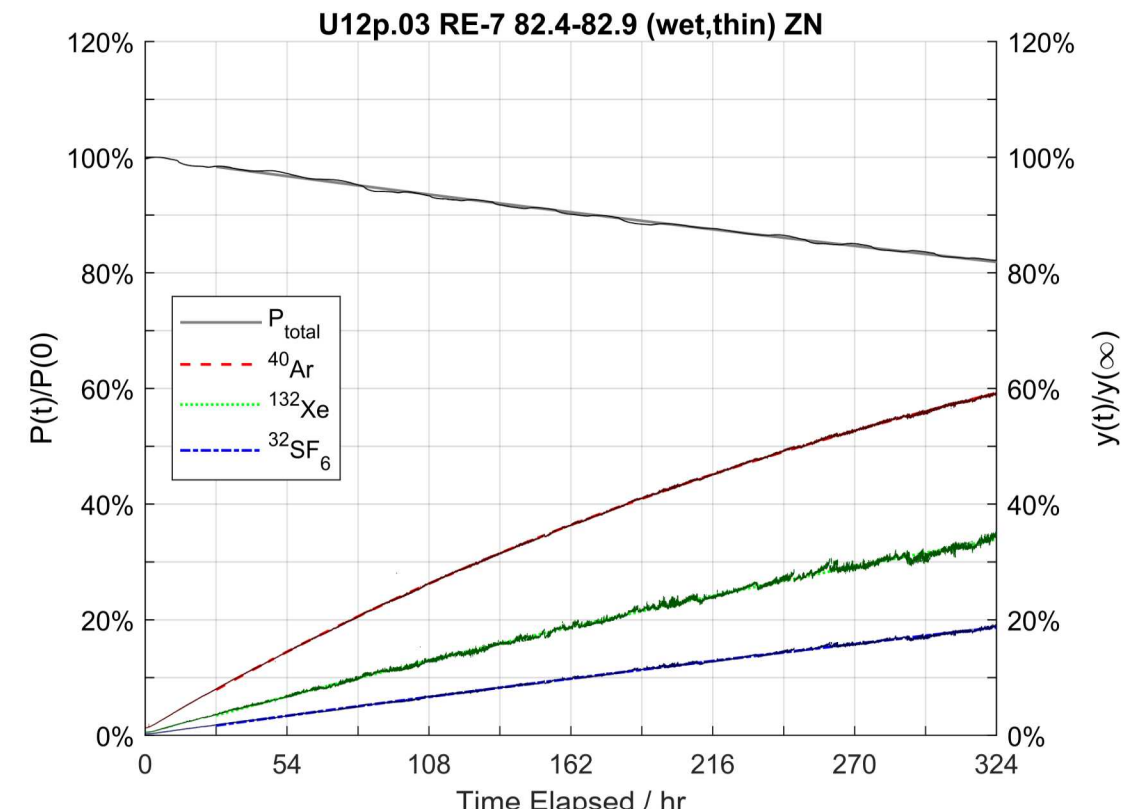
$$\begin{bmatrix} y_{i,\ell}(t) \\ y_{i,u}(t) \end{bmatrix} = y_{i,\infty} \begin{bmatrix} 1 \\ 1 \end{bmatrix} + y_{i,\Delta} \begin{bmatrix} -\mathfrak{D}_i \frac{A}{L} \frac{1}{V_\ell} \\ k_q \frac{V_\ell}{V_u} + \mathfrak{D}_i \frac{A}{L} \frac{1}{V_u} \end{bmatrix} e^{-k_{i,\Delta} t}$$

$$k_{i,\Delta} = k_q \frac{V_\ell}{V_u} + \mathfrak{D}_i \frac{A}{L} \left(\frac{1}{V_\ell} + \frac{1}{V_u} \right)$$

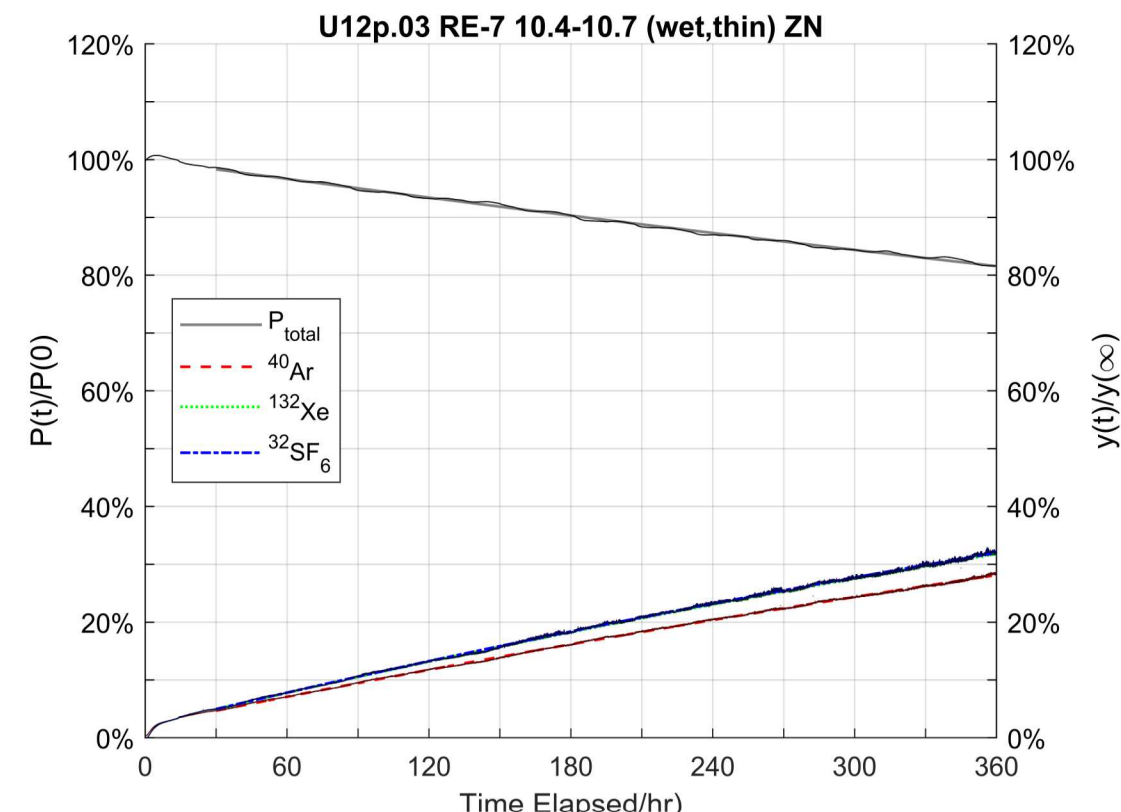
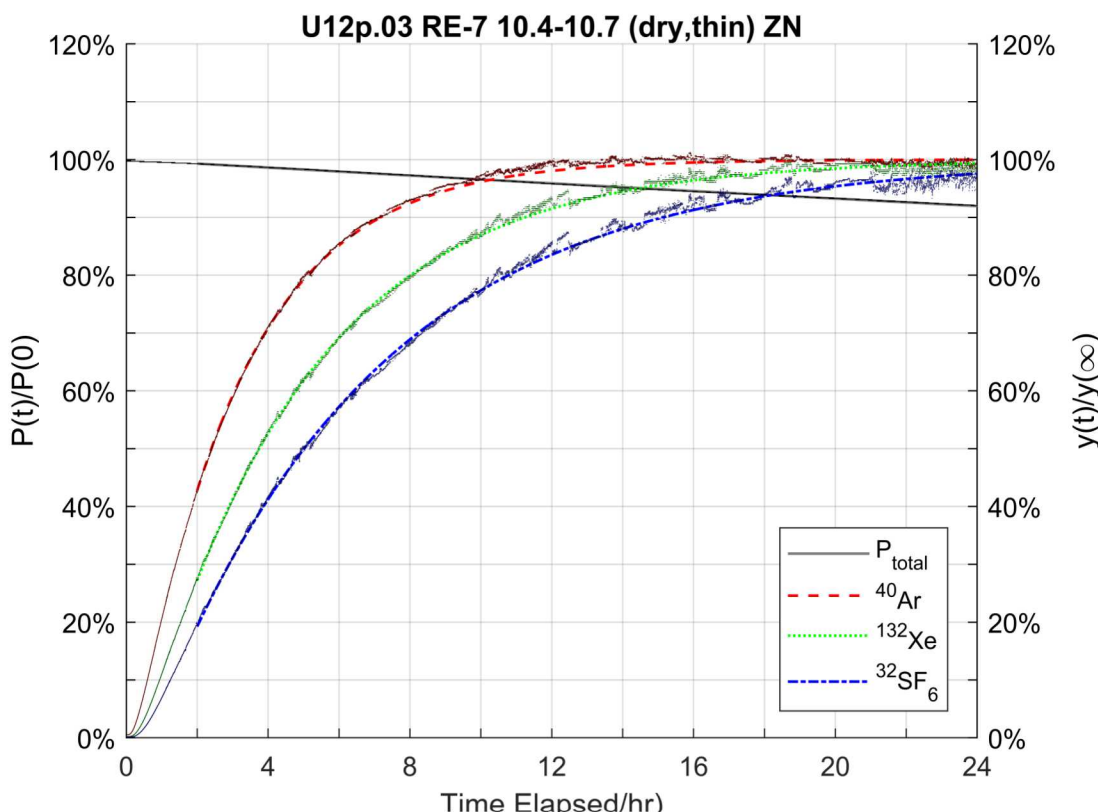
Paul, M.J. and S. T. Broome 2019. *Diffusive Properties of UNESE Core Samples via Continuously Monitored Mass Spectroscopy*. SAND2019-0786.



- Slow pressure decay – rapid concentration decay
- Curvature proportional to diffusivity



- Larger pressure decay – slower concentration decay
- Less curvature results in greater uncertainty



- **Electronic noise evident**
 - Random fluctuations mitigated by large data set

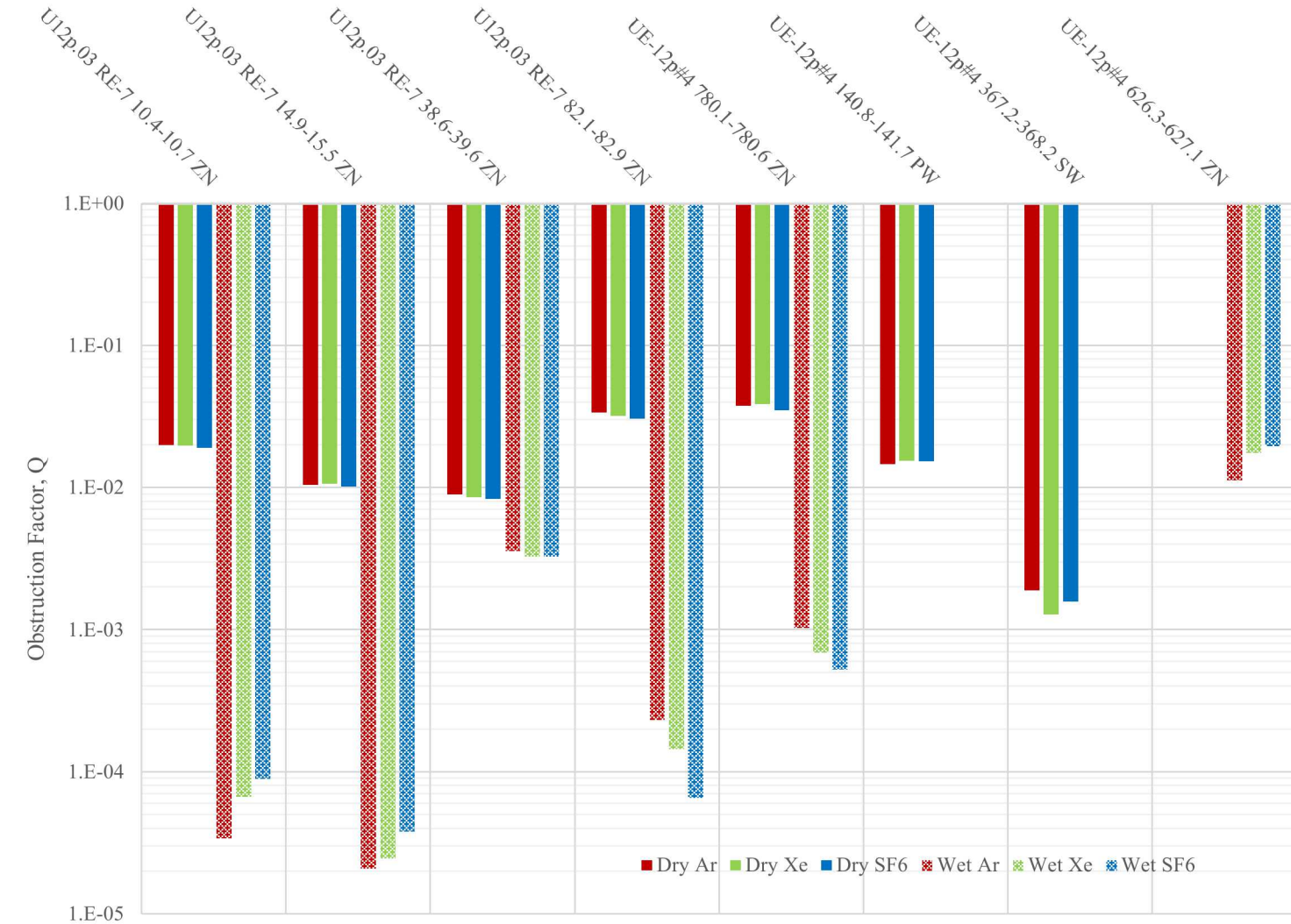
- **Pressure decay comparable to concentration decay**
- **Little to no curvature**
 - Inversion of ^{40}Ar and SF_6 suggest Taylor-Aris dispersion

Compiled UNESE Core Results

Testing species independent
obstruction factor
hypothesis:

$$Q_i = \frac{1}{D_{iN_2}} \frac{k_{i,\Delta} - k_q}{L} \frac{V_\ell}{V_u}$$

- $Q(\text{Ar}) = Q(\text{Xe}) = Q(\text{SF}_6)$
Obstruction factor is
independent
- $Q(\text{Ar}) < Q(\text{Xe}) < Q(\text{SF}_6)$
Deviation consistent with
Taylor dispersion
- Uncertainty is higher in
tighter media, obscuring
any surface effects



Conclusions

- The obstruction factor dominates in the lithologies considered here
- At the low end, some deviations have been observed, however:
 - There is considerably more numerical uncertainty at the low end,
 - Taylor dispersion may be occurring in microfractures, and/or
 - Surface diffusion may be occurring in micropores.
- The capability developed here is:
 - Applicable to a broad range of gases and vapors, including stable isotopes
 - Suitable for partially saturated media

Technical Challenges:

- **Very tight media have extended runtimes that may not be practical**
 - There is a limit where the matrix diffusivity becomes insignificant to radionuclide transport
- **The steady-state diffusivity may not be identical to the transient diffusive flux**
 - E.g. cul-de sac contribute to oscillatory flow not to steady-state transport

Future Work/Deliverables:

- **Acquire Hg-intrusion porosimetry data to estimate**
 - Capillary pressure curve
 - Estimate relative permeability and validate models on relevant lithologies
 - Correlate pore size distribution to diffusivity
- **Iterate on the continuous mass spectrometry design to:**
 - Modify system geometry shorten sample runtime
 - Reduce Taylor dispersion effects
 - Compare isotope specific diffusivities

Acknowledgements

- The authors acknowledge the support of the National Nuclear Security Administration Office of Defense Nuclear Nonproliferation Research and Development for funding this work.
- Sandia National Laboratories is a multi-mission laboratory managed and operated by National Technology & Engineering Solutions of Sandia, LLC, a wholly owned subsidiary of Honeywell International Inc., for the U.S. Department of Energy's National Nuclear Security Administration under contract DE-NA0003525.